Supplementary Materials 1

- **Types of engine damage caused by atmospheric mineral dusts**

Based on observation of engines during maintenance and on the results of engine tests, the types of engine damage caused by atmospheric mineral dusts may be categorised as:
(1) Impact erosion of engine parts
(2) Blockage of the intricate systems that deliver air for cooling and sealing within the engine
(3) Accumulation of deposits that effectively change the shape of engine parts and thereby reduce their aerodynamic efficiency
(4) Chemical and mechanical interactions between the deposits and engine components and protective coatings
(5) Mechanical damage to protective coatings during shedding.

A combination of these damage mechanisms can increase the damage considerably. For example, when the dust particles create an eroded surface, the fresh metal alloy substrate is subjected to continuous corrosion and deposition attack.

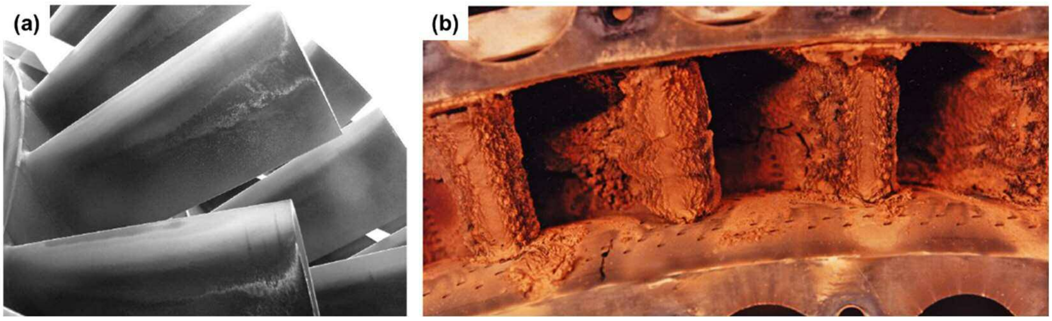

Supplementary Fig 1. *Engine environmental damages. (a) Solid particle deposits on a compressor rotor blade (Kurz and Brun, 2012). (b) Deposits formed on engine high pressure turbine vane (Dunn, 2012)*

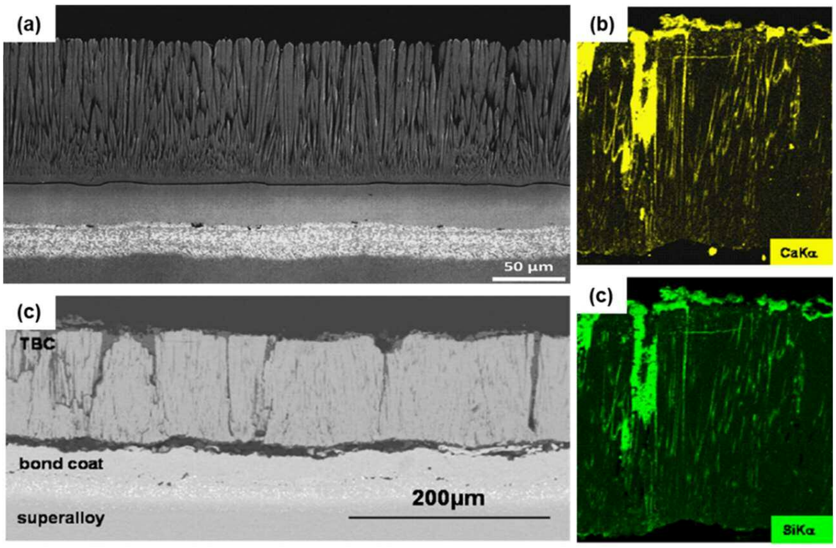

Supplementary Fig. 2. *Dust deposition influences on thermal barrier coatings (TBC) on engine blades and vanes. (a) columnar-shaped TBC microstructure. (b) and (c) showing the traces of CMAS compositions in the deposits and infiltrations. (d) is the TBC microstructure after CMAS deposition and infiltrations (Nieto et al., 2018, Mauer and Vaßen, 2019).*

Supplementary Materials 2

- **Why is fast scanning possible?**

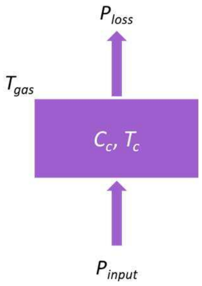

$$P_{loss} = -\frac{T_c - T_{gas}}{R_{CG}} \qquad P_{input} = C_c \cdot \beta$$

$$\beta\uparrow = -\frac{T_c - T_{gas}}{R_{CG}\downarrow \cdot C_c\downarrow}$$

a) Sufficiently low value of thermal resistance between calorimeter and gas → smaller sensor

b) Small heat capacity → thin Si_3N_x (x = 2.72–3.21) membrane

c) For cooling rates, necessarily surrounded by cold gas (T_{gas}↓).

- **Data calibration for thermal lag effects**

Flash DSC operates in power-compensated mode and use micro-electro-mechanical sensors (MEMS). There is a thermal lag determined exclusively by the sample and its contact to the sensor. The onset temperature T_{onest} and heating rate β are expected to show a linear relationship according to:

$$T_{onset} = T_{onset,\ 0\,K/s} + \tau_{lag}\beta$$

where $T_{onset,\ 0\,K/s}$ is the onset temperature extrapolated to a heating rate of 0 K/s. Here we used standard materials to conduct thermal lag calibrations and apply them to relevant experiments.

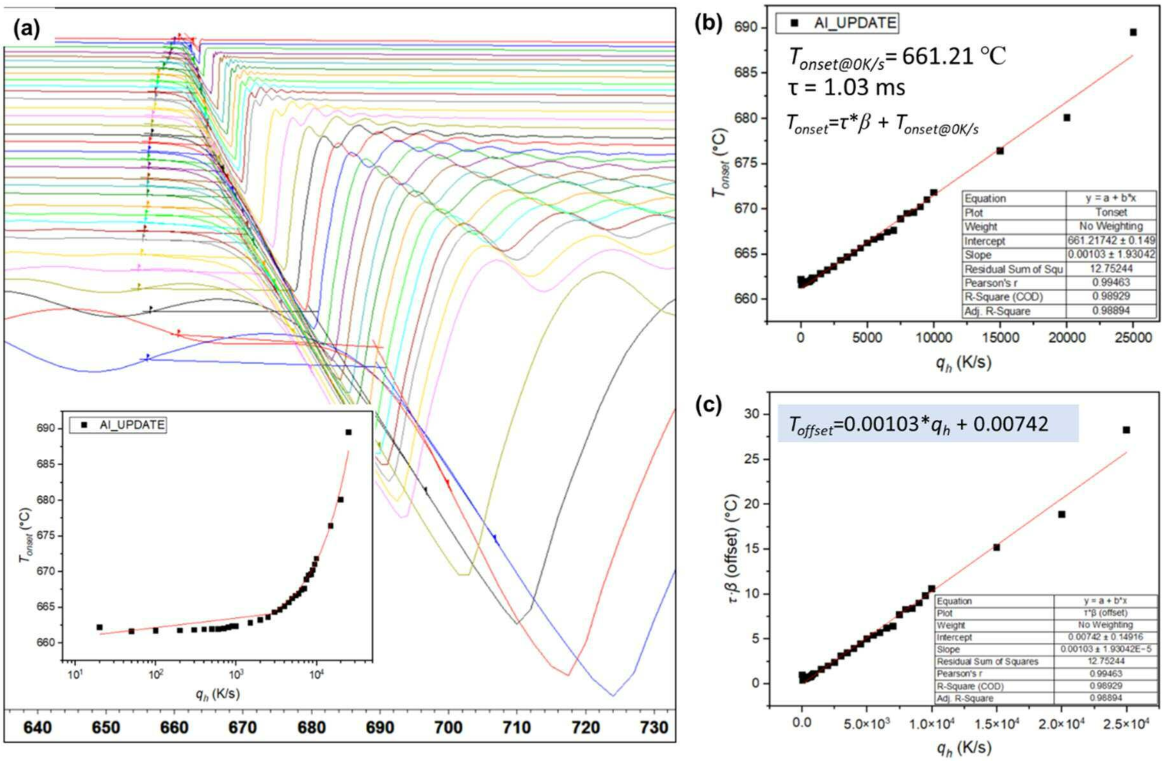

Supplementary Fig. 3. *Thermal lag calibration of Aluminium standard material. (a) Stack of Flash DSC heat flow vs. temperature curves showing the endothermic peak for melting at heating rates (q_h) between 1 and 30000 K/s. (b) is the relation between T_{onset} and q_h extracted from this peak, $T_{onset,\ 0\,K/s}$ is the extrapolation of this linear fit. (c) plot of offset temperature vs. q_h, this could then be applied to experimental data.*

Supplementary Material 3

Explained – fictive temperature (T_f)

- **How it is defined**

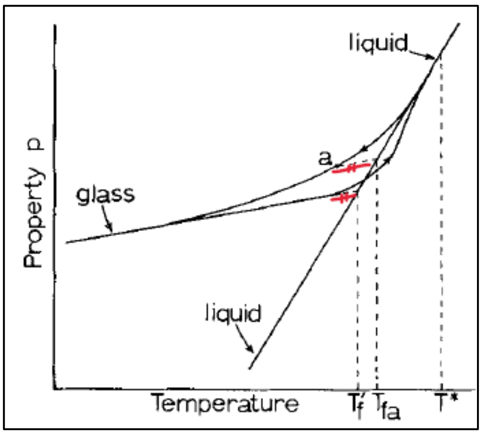

Within glassy phases there may be a range of structural reconfigurations during heating up to the melting temperature (or cooling from the melting temperature). These reconfigurations allow so-called "fictive temperatures" to be defined. **A fictive temperature is the temperature at which a metastable glass would find itself in equilibrium if suddenly brought to that temperature from some cooler temperature** (Datye et al., 2020). Hence each structural transformation has an accompanying fictive temperature. The measurement of fictive temperatures by thermal analysis can be used to ascertain cooling rates of quenched glasses, such as, the vitreous components of volcanic ash clouds (Scarani et al., 2022).

- **Approach to derive T_f**

The fictive temperature range can be determined with calorimetric measurements because the sample releases some excess in heat capacity when it is heated from the glass field into the liquid field. A unified area-matching method is used to derive T_f. Sample was subjected to a heating run, followed by a cooling run of the same rate, after which a second heating run was performed on this relaxed glass using a different rate. T_f of this unmatching cycle ($q_h \neq q_c$) was estimated according to:

$$\int_{T_{onset}}^{T_f} (C \quad _P) dT = \int_0^{\infty} (C_{P2} - C_{P2}) T$$

where C_{p2} and C_{p1} are the normalised excess heat capacity of the matching and unmatching cycle, respectively. Is the configurational heat capacity at T_g. The area difference between C_{p2} and C_{p1} corresponds to the rectangle area, hence Tf can be derived from there.

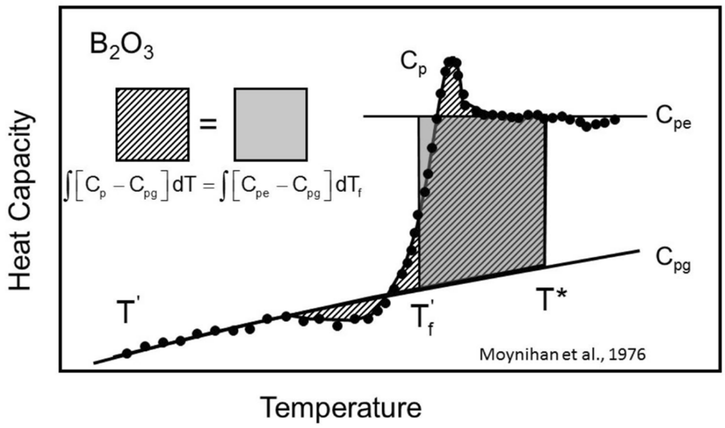

Supplementary Fig. 4. *Graphical representation of unified area-matching method, as found in Moynihan et al. 1976, showing the two integrals which need to equal to each other to determine the fictive temperature.*